

Frequency-dependent counting statistics in interacting nanoscale conductors

C. Emary,¹ D. Marcos,² R. Aguado,² and T. Brandes¹

¹*Institut für Theoretische Physik, Hardenbergstr. 36, TU Berlin, D-10623 Berlin, Germany*

²*Departamento de Teoría de la Materia Condensada, Instituto de Ciencia de Materiales de Madrid, CSIC, Cantoblanco 28049, Madrid, Spain*

(Received 21 August 2007; published 18 October 2007)

We present a formalism to calculate finite-frequency current correlations in interacting nanoscopic conductors. We work within the n -resolved density matrix approach and obtain a multitime cumulant generating function that provides the fluctuation statistics solely from the spectral decomposition of the Liouvillian. We apply the method to the frequency-dependent third cumulant of the current through a single resonant level and through a double quantum dot. Our results, which show that deviations from Poissonian behavior strongly depend on frequency, demonstrate the importance of finite-frequency higher-order cumulants in fully characterizing transport.

DOI: [10.1103/PhysRevB.76.161404](https://doi.org/10.1103/PhysRevB.76.161404)

PACS number(s): 73.23.Hk, 02.50.-r, 03.65.Yz, 72.70.+m

Following the considerable success of shot noise in the understanding of transport through mesoscopic systems,¹ attention is now turning towards the higher-order statistics of electron current. The so-called full counting statistics (FCS) of electron transport yields all moments (or cumulants) of the probability distribution $P(n, t)$ of the number of transferred electrons during time t . Despite their difficulty, measurements of the third moment of voltage fluctuations have been made,^{2,3} and recent developments in single electron detection^{4–6} promise to open new horizons on the experimental side.

The theory of FCS is now well established in the zero-frequency limit.^{7–9} However, this is by no means the full picture, since the higher-order current correlators at finite frequencies contain much more information than their zero-frequency counterparts. Already at second order (shot noise), one can extract valuable information about transport time scales and correlations. When the conductor has various intrinsic time scales like, for example, the charge relaxation time and the dwelling time of a chaotic cavity,¹⁰ one needs to go beyond second-order in order to fully characterize electronic transport. Apart from this example, and some other notable exceptions,^{11–13} the behavior of finite-frequency correlators beyond shot-noise is still largely unexplored.

In this Rapid Communication, we develop a theory of frequency-dependent current correlators of arbitrary order in the context of the n -resolved density matrix (DM) approach—a quantum optics technique¹⁴ that has recently found application in mesoscopic transport.¹⁵ Within this approach, the DM of the system, $\rho(t)$, is unravelled into components $\rho^{(n)}(t)$ in which $n=n(t)=0, 1, \dots$ electrons have been transferred to the collector. Considering a generic mesoscopic system with Hamiltonian $\mathcal{H}=\mathcal{H}_S+\mathcal{H}_L+\mathcal{H}_T$, where \mathcal{H}_S and \mathcal{H}_L refer to the system and leads, respectively, and provided that the Born-Markov approximation with respect to the tunnelling term \mathcal{H}_T is fulfilled, the time evolution of this n -resolved DM can be written quite generally as

$$\dot{\rho}^{(n)}(t) = \mathcal{L}_0 \rho^{(n)}(t) + \mathcal{L}_J \rho^{(n-1)}(t), \quad (1)$$

where the vector $\rho^{(n)}(t)$ contains the nonzero elements of the DM, written in a suitable many-body basis. The Liouvillian

\mathcal{L}_0 describes the “continuous” evolution of the system, whereas \mathcal{L}_J describes the quantum jumps of the transfer of an electron to the collector. We make the infinite bias voltage approximation such that the transfer is unidirectional. By construction, this method is very powerful for studying interacting mesoscopic systems that are weakly coupled to the reservoirs, such as coupled quantum dots (QDs) in the Coulomb blockade (CB) regime^{9,15,16} or Cooper-pair boxes.¹⁷ Within this framework, our theory of frequency-dependent FCS is of complete generality and therefore of wide applicability.

In this n -resolved picture, electrons are transferred to the leads via quantum jumps and there exists no quantum coherence between states in the system and those in the leads. Thus, although the system itself may be quantum, the measured current may be considered a classical stochastic variable and therefore amenable to classical counting.¹⁸ This observation allows us to derive various generalizations of classical stochastic results, and obtain a multitime cumulant generating function in terms of local propagators. We illustrate our method by calculating the frequency-resolved third cumulant (skewness) for two paradigms of CB mesoscopic transport: The single resonant level (SRL) and the double quantum dot (DQD).

Equation (1) can be solved by Fourier transformation. Defining $\rho(\chi, t) = \sum_n \rho^{(n)}(t) e^{in\chi}$, we obtain $\dot{\rho}(\chi, t) = M(\chi) \rho(\chi, t)$, with $M(\chi) \equiv \mathcal{L}_0 + e^{i\chi} \mathcal{L}_J$. Let N_v be the dimension of $M(\chi)$, and $\lambda_i(\chi)$; $i=1, \dots, N_v$, its eigenvalues. In the $\chi \rightarrow 0$ limit, one of these eigenvalues, $\lambda_1(\chi)$ say, tends to zero and the corresponding eigenvector gives the stationary DM for the system. This single eigenvalue is sufficient to determine the zero-frequency FCS.⁹ In contrast, here we need all N_v eigenvalues. Using the spectral decomposition, $M(\chi) = V(\chi) \Lambda(\chi) V^{-1}(\chi)$, with $\Lambda(\chi)$ the diagonal matrix of eigenvalues and $V(\chi)$ the corresponding matrix of eigenvectors, the DM of the system at an arbitrary time t is given by

$$\rho(\chi, t) = \Omega(\chi, t - t_0) \rho(\chi, t_0), \quad (2)$$

where $\Omega(\chi; t) \equiv e^{M(\chi)t} = V(\chi) e^{\Lambda(\chi)t} V^{-1}(\chi)$ is the propagator in χ space and $\rho(\chi, t_0)$ is the (normalized) state of the system at

t_0 , at which time we assume no electrons have passed so that $\boldsymbol{\rho}^{(n)}(t_0) = \delta_{n,0}\boldsymbol{\rho}(t_0)$ and thus $\boldsymbol{\rho}(\chi, t_0) \equiv \boldsymbol{\rho}(t_0)$. The propagator in n -space, $G(n, t) \equiv \int (d\chi/2\pi) e^{-in\chi} \Omega(\chi, t)$, such that $\boldsymbol{\rho}^{(n)}(t) = G(n, t-t_0)\boldsymbol{\rho}(t_0)$, for $t > t_0$, fulfills the property: $G(n-n_0, t-t_0) = \sum_{n'} G(n-n', t-t') G(n'-n_0, t'-t_0)$, for $t > t' > t_0$ [$n' \equiv n(t')$, $n_0 \equiv n(t_0)$]. This is an operator version of the Chapman-Kolmogorov equation.¹⁹

The joint probability of obtaining n_1 electrons after t_1 and n_2 electrons after t_2 , namely $P^>(n_1, t_1; n_2, t_2)$ (the superscript “>” implies $t_2 > t_1$), can be written in terms of these propagators by evolving the local probabilities $P(n, t) = \text{Tr}\{\boldsymbol{\rho}^{(n)}(t)\}$,²⁰ and taking into account $P(n_2, t_2) = \sum_{n_1} P^>(n_1, t_1; n_2, t_2)$, such that

$$P^>(n_1, t_1; n_2, t_2) = \text{Tr}[G(n_2 - n_1, t_2 - t_1) G(n_1, t_1 - t_0)\boldsymbol{\rho}(t_0)]. \quad (3)$$

The total joint probability reads

$$P(n_1, t_1; n_2, t_2) = \mathcal{T}P^>(n_1, t_1; n_2, t_2) = P^>(n_1, t_1; n_2, t_2)\theta(t_2 - t_1) + P^<(n_1, t_1; n_2, t_2)\theta(t_1 - t_2),$$

where \mathcal{T} is the time-ordering operator, $\theta(t)$ the unit step function defined as $\theta(t) = 1$ for $t \geq 0$, and zero otherwise, and where $P^<(n_1, t_1; n_2, t_2)$ is the joint probability with $t_2 < t_1$. It should be noted that, in contrast to the local probability $P(n, t)$, the joint probability $P(n_1, t_1; n_2, t_2)$ contains information about the correlations at *different times*.

Result (3) may be alternatively derived using the Bayes formula for the conditional density operator:²¹

$$P^>(n_1, t_1; n_2, t_2) = P(n_1, t_1)P^>(n_2, t_2|n_1, t_1) = \text{Tr}\{\boldsymbol{\rho}^{(n_1)}(t_1)\} \times \text{Tr}\{\boldsymbol{\rho}^{(n_2|n_1)}(t_2)\} = \text{Tr}\{\boldsymbol{\rho}^{(n_1)}(t_1)\} \times \text{Tr}\left\{G(n_2 - n_1, t_2 - t_1) \frac{\boldsymbol{\rho}^{(n_1)}(t_1)}{\text{Tr}\{\boldsymbol{\rho}^{(n_1)}(t_1)\}}\right\}.$$

The normalization in the denominator accounts for the collapse $n = n_1$ at $t = t_1$ using Von Neumann’s projection postulate.²¹ Equation (3) is recovered when $\boldsymbol{\rho}^{(n_1)}(t_1)$ is written as a time evolution from t_0 .

The two-time cumulant generating function (CGF) associated with these joint probabilities is

$$e^{-\mathcal{F}(\chi_1, \chi_2; t_1, t_2)} \equiv \sum_{n_1, n_2} P(n_1, t_1; n_2, t_2) e^{in_1\chi_1 + in_2\chi_2},$$

which, using Eq. (3), and $e^{-\mathcal{F}} = e^{-\mathcal{TF}^>} = \mathcal{T}e^{-\mathcal{F}^>}$, gives

$$e^{-\mathcal{F}(\chi_2, \chi_1; t_2, t_1)} = \mathcal{T} \text{Tr}[\Omega(\chi_2, t_2 - t_1) \times \Omega(\chi_1 + \chi_2, t_1 - t_0)\boldsymbol{\rho}(t_0)]. \quad (4)$$

The above procedure can be easily generalized to obtain the N -time CGF, which reads

$$e^{-\mathcal{F}(\boldsymbol{\chi}; \boldsymbol{t})} = \mathcal{T} \text{Tr}\left\{\prod_{k=1}^N \Omega(\sigma_k; \tau_{N-k})\boldsymbol{\rho}(t_0)\right\}, \quad (5)$$

where $\sigma_k \equiv \sum_{i=N+1-k}^N \chi_i$, $\boldsymbol{\chi} \equiv (\chi_1, \dots, \chi_N)$, $\boldsymbol{t} \equiv (t_1, \dots, t_N)$, and $\tau_k \equiv t_{k+1} - t_k$.²² The multitime CGF in Eq. (5) contains a product of local-time propagators, and expresses the Markovian

character of the problem. It allows one to obtain all the frequency-dependent cumulants from the spectral decomposition of $M(\chi)$. The N -time current-cumulant ($e=1$) is calculated using

$$\begin{aligned} S^{(N)}(t_1, \dots, t_N) &\equiv \langle \delta I(t_1) \dots \delta I(t_N) \rangle \\ &= \partial_{t_1} \dots \partial_{t_N} \langle n(t_1) \dots n(t_N) \rangle \\ &= -(-i)^N \partial_{t_1} \dots \partial_{t_N} \partial_{\chi_1} \dots \partial_{\chi_N} \mathcal{F}(\boldsymbol{\chi}; \boldsymbol{t}) \Big|_{\boldsymbol{\chi}=\mathbf{0}}. \end{aligned} \quad (6)$$

The Fourier transform of $S^{(N)}$ with respect to the time intervals τ_k , gives the N th-order correlation functions as functions of $N-1$ frequencies. In particular, the frequency-dependent skewness is a function of two frequencies which, as a consequence of time-symmetrization and the Markovian approximation, has the symmetries $S^{(3)}(\omega, \omega') = S^{(3)}(\omega', \omega) = S^{(3)}(\omega, \omega - \omega') = S^{(3)}(\omega' - \omega, \omega') = S^{(3)}(-\omega, -\omega')$, and is therefore real. The N th-order Fano factor is defined as $F^{(N)} \equiv S^{(N)}/\langle I \rangle$.

In the case where the jump matrix \mathcal{L}_J contains a single element, $(\mathcal{L}_J)_{ij} = \Gamma_R \delta_{i\alpha} \delta_{j\beta}$, which is the case for a wide class of models including our two examples below, all the correlation functions can be expressed solely in terms of the eigenvalues λ_k of $M(0)$, and the N_v coefficients $c_k \equiv (V^{-1} \mathcal{L}_J V)_{kk} = \Gamma_R V_{\beta k} V_{k\alpha}^{-1}$. The second-order Fano factor then has the simple, general form

$$F^{(2)}(\omega) = 1 - 2 \sum_{k=2}^{N_v} \frac{c_k \lambda_k}{\omega^2 + \lambda_k^2}, \quad (7)$$

which has also been derived in other ways.²³ The skewness has the form $F^{(3)}(\omega, \omega') = -2 + \sum_{i=1}^3 F^{(2)}(\nu_i) + \tilde{F}^{(3)}(\omega, \omega')$, with $\nu_1 = \omega$, $\nu_2 = \omega'$, and $\nu_3 = \omega - \omega'$. $\tilde{F}^{(3)}(\omega, \omega')$ is an irreducible contribution, the form of which is too cumbersome to be given here. The high-frequency limit of the skewness is $F^{(3)}(\omega, \infty) = F^{(2)}(\omega)$.

As a first example, we consider a SRL described by $\boldsymbol{\rho} = (\rho_{00}, \rho_{11})^T$ and

$$M(\chi) = \begin{pmatrix} -\Gamma_L & e^{i\chi}\Gamma_R \\ \Gamma_L & -\Gamma_R \end{pmatrix},$$

in the basis of “empty” and “populated” states, $\{|0\rangle, |1\rangle\}$. Employing Eq. (5), we obtain the known results for the current and noise, and arrive at our result for the skewness:

$$F^{(3)}(\omega, \omega') = 1 - 2\Gamma_L\Gamma_R \frac{\prod_{i=1}^2 (\gamma_i + \omega^2 - \omega\omega' + \omega'^2)}{\prod_{j=1}^3 (\Gamma^2 + \nu_j^2)},$$

with $\gamma_1 = \Gamma_L^2 + \Gamma_R^2$, $\gamma_2 = 3\Gamma^2$, and $\Gamma = \Gamma_L + \Gamma_R$. The zero-frequency limit $F^{(3)}(0, 0)$ is in accordance with Ref. 24.

This skewness is plotted in Fig. 1, from which the sixfold symmetry of $F^{(3)}$ is readily apparent. The third-order Fano factor gives, in accordance with the noise, a sub-Poissonian behavior for all frequencies. This can be easily understood as a CB suppression of the long tail of the probability distribution of instantaneous current: Due to the infinite bias, the

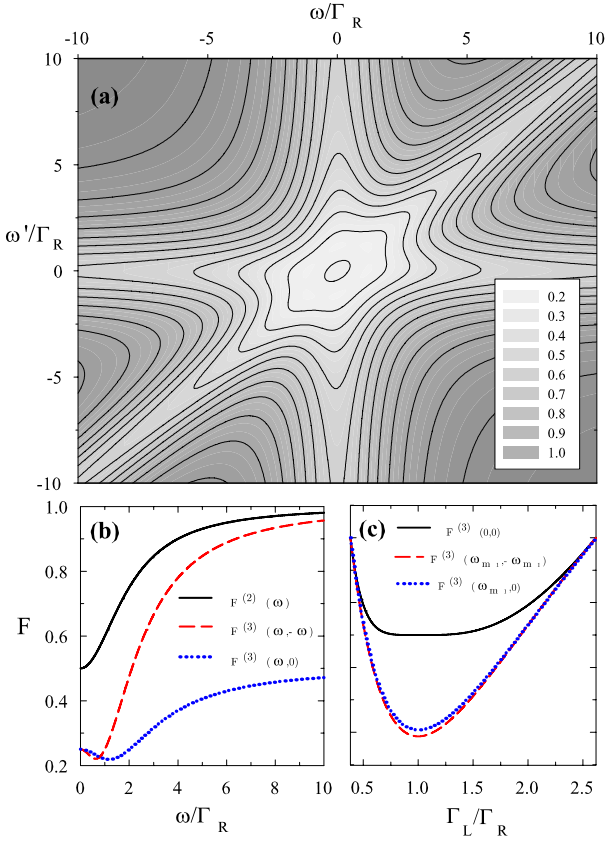


FIG. 1. (Color online) The third-order frequency-dependent Fano factor $F^{(3)}(\omega, \omega')$ for the single resonant level. (a) Contour plot of $F^{(3)}(\omega, \omega')$ as a function of its arguments for $\Gamma_R = \Gamma_L$. (b) Sections $F^{(3)}(\omega, 0)$ and $F^{(3)}(\omega, -\omega)$ show that the skewness is suppressed throughout frequency space both with respect to the Poissonian value of unity and to the noise $F^{(2)}(\omega)$. In contrast to the shotnoise, the skewness has a minimum at a finite frequency ω_m , which exists in the coupling range $(3 - \sqrt{5})/2 \leq \Gamma_L/\Gamma_R \leq (3 + \sqrt{5})/2$. In direction $\omega = -\omega'$, this minimum occurs, for $\Gamma_L = \Gamma_R$, at $\omega_{m1}/\Gamma_R = \sqrt{10 - 2}/\sqrt{3}$ whereas for $\omega' = 0$ the position of the minimum shifts slightly to $\omega_{m2}/\Gamma_R = 2/\sqrt{3}$. (c) The maximum suppression occurs at $\Gamma_L = \Gamma_R$.

distribution is bounded on the left by zero, but, in principle, is not bounded on the right (large, positive skewness). CB suppresses large current fluctuations which explains a sub-Poissonian skewness.

Along the symmetry lines in frequency space with $\omega' = 0$, $\omega' = \omega$, and $\omega = 0$, the skewness is highly suppressed. In contrast with the noise, the minimum in the skewness occurs at finite frequency [Fig. 1(b)] with the strongest suppression occurring at $\Gamma_L = \Gamma_R$ [Fig. 1(c)].

As a second example, we consider a DQD in the strong CB regime.^{25,26} In the basis of “left” and “right” states $|L\rangle$ and $|R\rangle$, which denote states with one excess electron with respect to the many body “empty” state $|0\rangle$, the Hamiltonian reads $\mathcal{H}_S = \epsilon(|L\rangle\langle L| - |R\rangle\langle R|) + T_c(|L\rangle\langle R| + |R\rangle\langle L|)$, with detuning ϵ and coupling strength T_c . The two levels $|L\rangle, |R\rangle$, are coupled to their respective leads with rates Γ_L and Γ_R . The DM vector is now $\boldsymbol{\rho} = [\rho_{00}, \rho_{LL}, \rho_{RR}, \text{Re}(\rho_{LR}), \text{Im}(\rho_{LR})]^T$, and the Liouvillian in this basis reads

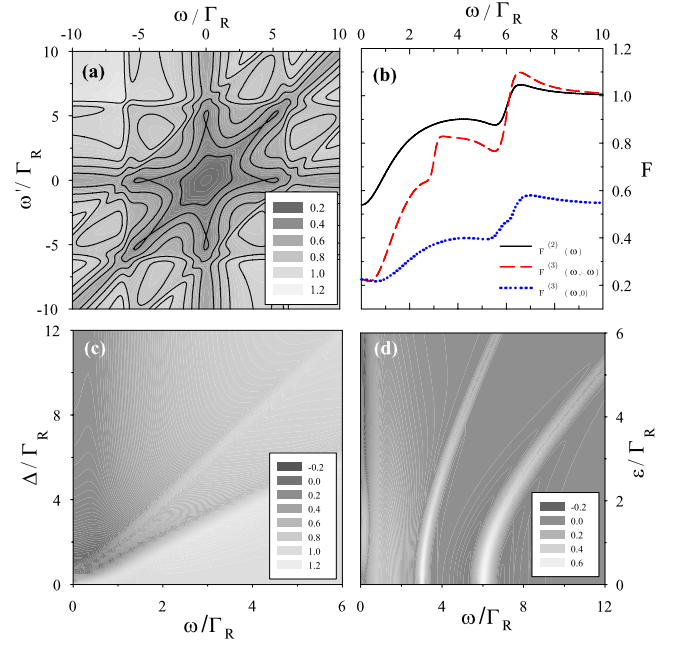


FIG. 2. (Color online) Frequency-dependent Fano skewness for the double quantum dot in Coulomb blockade. (a) Contour plot in the strong coupling regime, $T_c = 3\Gamma_R$, with $\Gamma_L = \Gamma_R$ and $\epsilon = 0$. (b) Sections $F^{(3)}(\omega, 0)$ and $F^{(3)}(\omega, -\omega)$, and shot noise $F^{(2)}(\omega)$ show a series of abrupt increases with increasing ω . Both noise and skewness exhibit both sub- and super-Poissonian behavior. (c) Varying the internal coupling T_c , the skewness shows rapid increases along the lines $\omega = \Delta$ and $\omega = \Delta/2$. For $\omega > \Delta$ the system is Poissonian (slightly super-Poissonian for $\omega \gtrsim \Delta$), while for $\omega < \Delta$ the transport is always sub-Poissonian. The skewness is strongly suppressed at low frequencies. (d) The derivative $dF^{(3)}(\omega, -\omega)/d\omega$ as a function of frequency and detuning ϵ for $T_c = 3\Gamma_L = 3\Gamma_R$. Resonances occur at $\omega = \Delta, \Delta/2$, and $-\Gamma_R$.

$$M(\chi) = \begin{pmatrix} -\Gamma_L & 0 & e^{i\chi}\Gamma_R & 0 & 0 \\ \Gamma_L & 0 & 0 & 0 & -2T_c \\ 0 & 0 & -\Gamma_R & 0 & 2T_c \\ 0 & 0 & 0 & -\frac{1}{2}\Gamma_R & 2\epsilon \\ 0 & T_c & -T_c & -2\epsilon & -\frac{1}{2}\Gamma_R \end{pmatrix}.$$

Comparison of the quantum-mechanical level-splitting $\Delta \equiv 2\sqrt{T_c^2 + \epsilon^2}$ with the incoherent rates $\Gamma_{L,R}$ divides the dynamical behavior of the system into two regimes. For $\Delta \ll \Gamma_{L,R}$, all eigenvalues of $M(0)$ are real, and correspondingly, the noise and skewness are slowly varying functions of their frequency arguments. In this regime, dephasing induced by the leads suppresses interdot coherence, and the transport is largely incoherent. In the opposite regime, $\Delta \gg \Gamma_{L,R}$, two of the eigenvalues form a complex pair, $\lambda_{\pm} \approx \pm i\Delta - \Gamma_R/2 + O(\Gamma/\Delta)^2$, which signals the persistence of coherent oscillations in the dots. The finite-frequency correlators then show resonant features at Δ , since these eigenvalues enter into the denominators, as in Eq. (7), giving rise to poles such as $\omega \mp \Delta - i\Gamma_R/2$. The structure of the skewness is similar to the SRL for weak coupling ($\Delta \ll \Gamma_{L,R}$), but much

richer in the strong coupling regime ($\Delta \gg \Gamma_{L,R}$) (Fig. 2). Now the skewness exhibits a series of rapid increases. From the origin outwards in the $\omega - \omega'$ plane, we observe first a minimum at finite frequency and then inflexion points at $\omega \sim \Gamma_R$, $|\omega| = \Delta$, $|\omega'| = \Delta$, and $|\omega - \omega'| = \Delta$. Figure 2(b) shows sections in the $\omega - \omega'$ plane, and the resonant behavior, in the form of Fano shapes, is most pronounced in $F^{(3)}(\omega, -\omega)$. Starting from high frequencies, the onset of antibunching occurs at $\omega = \Delta$. At higher frequencies, the system has no information about correlations and is Poissonian. The overall behavior is seen in Fig. 2(c) where we plot $F^{(3)}(\omega, -\omega)$ as a function of T_c and ω . The line $\omega = \Delta$ delimits two regions: At high frequencies the skewness is Poissonian. At resonance, and after a small super-Poissonian region at $\omega \gtrsim \Delta$, the system becomes sub-Poissonian (and even negative, for certain internal couplings). In the limit $\omega \rightarrow 0$, our results qualitatively agree with those of Ref. 27 for a noninteracting DQD: As a function of T_c , the skewness presents two minima and a maximum (where the noise is minimum, not shown). In our case, however, the maximum occurs around Δ

$= \Gamma_R/2$ —half that of the noninteracting case. Finally, we plot $dF^{(3)}(\omega, -\omega)/d\omega$ as a function of both ϵ and ω [Fig. 2(d)] where the resonances at $\omega = \Delta$, $\omega = \Delta/2$, and $\omega \sim \Gamma_R$ are clearly resolved. In contrast, the derivative $dF^{(3)}(\omega, 0)/d\omega$ (not shown), exhibits a minimum at $\omega = \Delta$ for small ϵ , which transforms into a maximum for $\epsilon \gg T_c$. As expected, transport tends to be more Poissonian as ϵ increases, signaling loss of coherence.

Despite the simplicity of the models we have studied, our results demonstrate the importance of finite-frequency studies. Deviations from Poissonian behavior of higher-order cumulants are frequency-dependent, such that a comprehensive analysis in the frequency domain is needed in order to fully characterize correlations and statistics in electronic transport.

Work was supported by the WE Heraeus foundation, DFG Grant No. BR 1528/5-1, and by Grants No. MAT2006-03741 and No. FPU AP2005-0720 (MEC-Spain), No. 20060I003 (CSIC), and No. 200650M047 (CAM).

-
- ¹Ya. M. Blanter and M. Buttiker, Phys. Rep. **336**, 1 (2000).
²B. Reulet, J. Senzier, and D. E. Prober, Phys. Rev. Lett. **91**, 196601 (2003).
³Yu. Bomze, G. Gershon, D. Shovkun, L. S. Levitov, and M. Reznikov, Phys. Rev. Lett. **95**, 176601 (2005).
⁴T. Fujisawa, T. Hayashi, R. Tomita, and Y. Hirayama, Science **312**, 1634 (2006).
⁵S. Gustavsson, R. Leturcq, B. Simovič, R. Schleser, T. Ihn, P. Studerus, K. Ensslin, D. C. Driscoll, and A. C. Gossard, Phys. Rev. Lett. **96**, 076605 (2006); S. Gustavsson, R. Leturcq, T. Ihn, K. Ensslin, M. Reinwald, and W. Wegscheider, Phys. Rev. B **75**, 075314 (2007).
⁶E. V. Sukhorukov, A. N. Jordan, S. Gustavsson, R. Leturcq, T. Ihn, and K. Ensslin, Nat. Phys. **3**, 243 (2007).
⁷L. S. Levitov and G. B. Lesovik, Pis'ma Zh. Eksp. Teor. Fiz. **58**, 225 (1993); L. S. Levitov, H.-W. Lee, and G. B. Lesovik, J. Math. Phys. **37**, 4845 (1996).
⁸Yu. V. Nazarov, Ann. Phys. **8**(special issue), SI-193 (1999).
⁹D. A. Bagrets and Yu. V. Nazarov, Phys. Rev. B **67**, 085316 (2003).
¹⁰K. E. Nagaev, S. Pilgram, and M. Büttiker, Phys. Rev. Lett. **92**, 176804 (2004).
¹¹S. Pilgram, K. E. Nagaev, and M. Buttiker, Phys. Rev. B **70**, 045304 (2004).
¹²A. V. Galaktionov, D. S. Golubev, and A. D. Zaikin, Phys. Rev. B **68**, 235333 (2003).
¹³J. Salo, F. W. J. Hekking, and J. P. Pekola, Phys. Rev. B **74**, 125427 (2006).
¹⁴R. J. Cook, Phys. Rev. A **23**, 1243 (1981).
¹⁵S. A. Gurvitz, Phys. Rev. B **57**, 6602 (1998).
¹⁶R. Aguado and T. Brandes, Phys. Rev. Lett. **92**, 206601 (2004).
¹⁷M.-S. Choi, F. Plastina, and R. Fazio, Phys. Rev. Lett. **87**, 116601 (2001).
¹⁸This is in contrast with quantum detection, where the noncommutativity of current at different times must be explicitly considered (Ref. 7).
¹⁹N. G. Van Kampen, *Stochastic Processes in Physics and Chemistry* (North-Holland P.L., Amsterdam, 1992).
²⁰With ρ a vector, the trace operation corresponds to a sum over all the diagonal elements of the original DM.
²¹A. N. Korotkov, Phys. Rev. B **63**, 115403 (2001).
²²One can also obtain the CGF in terms of a single *time-dependent* counting field from the expression $e^{-\mathcal{F}[\chi]} := \mathcal{G}[\chi] \equiv \langle e^{i \int n(t) \chi(t) dt} \rangle_{\mathcal{T}}$, where $\langle \dots \rangle_{\mathcal{T}}$ denotes a time-ordered path integral with the joint probability as the weight function (Ref. 9). Establishing the bisection between t and n , one recovers Eq. (5) in terms of products of evolution operators by dividing the time interval into subintervals $\tau_k := t_{k+1} - t_k$, $k=0, \dots, N-1$, with associated time-independent counting fields χ_k and variables n_k .
²³S. Hershfield, J. H. Davies, P. Hyldgaard, C. J. Stanton, and J. W. Wilkins, Phys. Rev. B **47**, 1967 (1993); C. Flindt, T. Novotný, and A.-P. Jauho, Physica E (Amsterdam) **29**, 411 (2005).
²⁴M. J. M. de Jong, Phys. Rev. B **54**, 8144 (1996).
²⁵T. H. Stoof and Yu. V. Nazarov, Phys. Rev. B **53**, 1050 (1996).
²⁶T. Brandes, Phys. Rep. **408**, 315 (2005).
²⁷G. Kiesslich, P. Samuelsson, A. Wacker, and E. Schöll, Phys. Rev. B **73**, 033312 (2006).